Hindawi Publishing Corporation
International Journal of Antennas and Propagation
Volume 2016, Article ID 9265159, 8 pages
http://dx.doi.org/10.1155/2016/9265159

Research Article

Experimental Study on Inkjet-Printed Passive UHF RFID Tags on Versatile Paper-Based Substrates

Han He, Lauri Sydänheimo, Johanna Virkki, and Leena Ukkonen

Department of Electronics and Communications Engineering, Tampere University of Technology, P.O. Box 692, 33101 Tampere, Finland

Correspondence should be addressed to Han He; han.he@tut.fi

Received 13 May 2016; Accepted 13 July 2016

Academic Editor: Rocco Guerriero

We present the possibilities and challenges of passive UHF RFID tag antennas manufactured by inkjet printing silver nanoparticle ink on versatile paper-based substrates. The most efficient manufacturing parameters, such as the pattern resolution, were determined and the optimal number of printed layers was evaluated for each substrate material. Next, inkjet-printed passive UHF RFID tags were fabricated on each substrate with the optimized parameters and number of layers. According to our measurements, the tags on different paper substrates showed peak read ranges of 4–6.5 meters and the tags on different cardboard substrates exhibited peak read ranges of 2–6 meters. Based on their wireless performance, these inkjet-printed paper-based passive UHF RFID tags are sufficient for many future wireless applications and comparable to tags fabricated on more traditional substrates, such as polyimide.

1. Introduction

The development of the Internet of Things has created a need for cost-effective wireless electronics on environmentally friendly substrates. Great potential lies especially in inkjet printing and inkjet-printed antennas [1–3]. Particularly RFID (radiofrequency identification) tag antennas printed on versatile substrates and the use of renewable substrate materials, such as paper and cardboard, provide endless opportunities. Paper and cardboard have a wide range of properties based on their composition; they can be flexible, rigid, soft, and coarse, and they may absorb or repel water. Paper and cardboard are also available with textured surfaces. These paper-based materials are indispensable materials in the packaging and graphics industry, which also makes them an interesting substrate material for printed RFID tag antennas [4–6]. However, the optimized printing parameters need to be studied first.

RFID technology is a wireless identification technology to automatically identify and track physical objects or people by using radiofrequency waves. When using RFID tags for identification, multiple devices can be read simultaneously and a line-of-sight is not necessary [7]. Passive UHF (ultra high frequency) RFID technology shows promise in embedded applications: passive tags require very little maintenance because no battery change is required. Also the read ranges of passive UHF RFID systems are longer compared to other RFID frequencies [8, 9]. The signal from the reader is necessary for a passive tag to power up the IC (integrated circuit) and reply to the reader.

The goal of this paper is to study the possibility of inkjet printing on various paper and cardboard substrates and to optimize the printing parameters in order to effectively fabricate passive UHF RFID tags on these substrates. The ready RFID tags are evaluated for their wireless performance and compared to tags fabricated on a more traditional polyimide substrate.

2. Manufacturing of Passive UHF RFID Tags

2.1. Material and Tools. The used ink was Harima NPS-JL silver nanoparticle ink [10] and the main specifications of the silver ink are shown in Table 1. In this study, the ink deposition was completed with Fujifilm Dimatix DMP-2831 material inkjet printer. A 10 pL volume cartridge,which has a

Table 1: Specifications of the utilized ink [10].

Ink	Ag NPS-JL NanoPaste®
Solid content (wt%)	52–57
Particle size (nm)	5–12
Average particle size (nm)	7
Resistivity ($\mu\Omega\cdot$cm)	4–6
Viscosity (mPa·s)	11.5 (measured at 20°C and 60 rpm)
Recommended thermal curing	120–150°C for 60 minutes

Table 2: Substrate properties.

Substrate	Thickness	Speciation
Paper A	100 μm	Uncoated paper
Paper B	80 μm	Coated, calendered
Paper C	80 μm	Double coated: film + blade
Cardboard A	500 μm	Double coated: film + blade
Cardboard B	500 μm	Base board

snap-in replaceable print head with 16 nozzles, was applied for ejecting the drops.

The substrate material plays a big role in additive RFID tag manufacturing. Different substrate materials need different printing parameters, because they have different surface properties and morphologies. In [5] the dielectric characteristics of paper were investigated in the UHF range and the relative permittivity (3.2–3.5) and loss tangent (0.006–0.008) of commercial paper were studied by using a microstrip ring resonator. It should also be noted that the reported values are not constant and, in addition to frequency, they will vary with, for example, temperature and humidity. In this study, several types of paper and cardboard materials were selected for inkjet printing and the properties (calendered/noncalendered, coated/noncoated) of these substrates are shown in Table 2. Furthermore, calendaring is a process that uses series of hard pressure rollers to form or smooth a sheet of material, such as paper or cardboard. A coating is a covering that is applied to the surface of the paper or cardboard by the manufacturer. With a glossy or matte finish, a coated substrate generally has very smooth surface and the coating can restrict the amount of ink that is absorbed by the substrate material. The substrates used in this experiment are blade coated and/or film coated.

2.2. Printing Parameters. There are several parameters that can affect the printing quality, such as the jetting pulse shape, the jetting frequency, the jetting voltage, and the temperature of the ink cartridge, as well as the pattern resolution. The used jetting pulse shape is shown in Figure 1. In this research, three active nozzles were used for inkjet printing. To ensure that the ink droplets jetted to each substrate attach well on the substrate surface, without unnecessary spreading, we did preliminary tests on droplets. Normally, the drop spacing, which decides the printing resolution, is defined as the distance between the centers of two adjacent droplets. On this printer, the drop spacing must be equal on both the X and

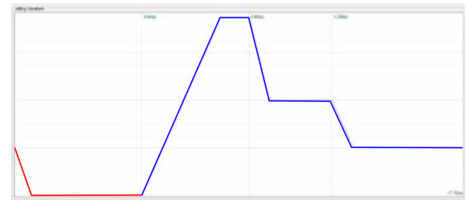

Figure 1: The used jetting pulse shape.

Y directions. On the X direction, the drop spacing is always set manually. On the Y direction, the drop spacing is defined by the cartridge tilt angle between the X direction (axe of displacement of the print carriage) and the axe of the nozzles, which are regularly spaced by 254 μm. An angle of 90° corresponds to the maximum achievable drop spacing (254 μm). Decreasing the drop spacing corresponds to increasing the pattern resolution. Depending on the interaction of the ink with the substrate, the drop size of the ink on different substrate materials can be different. Usually, the appropriate droplet spacing is equal to the radius of the drop, which can then decide the printing resolution. If the resolution is too low, the droplets may not overlap, while if the resolution is too high, overspreading of the ink might occur causing the loss of the pattern shape [11]. Figure 2 shows the microscope images of the silver nanoparticle ink droplets on all substrates, and the selected resolution of every substrate is listed in Table 3. In addition, Table 4 indicates the printing parameters, which were kept identical for all substrates.

2.3. Number of Printed Layers. After finding the optimized printing parameters, simple lines with dimensions of 5 mm × 30 mm were printed on each substrate to study the optimal number of layers. In theory, when the antenna design and the substrate are the same, antennas with better conductivity (lower DC resistance) should have higher read ranges. Based on the datasheet of the ink, the sintering was done at 150°C for 60 minutes to maximize the conductivity of the printed layer [10]. The resistances of the lines were measured from corner to corner using Fluke 111 True RMS Multimeter. The measurement was repeated 4 times and then the average value was calculated. The measured resistances are presented in Table 5. In addition, Figure 3 shows the printed line patterns on all substrates and the surface magnified images from optical microscope can be seen in Figure 4.

One-layer lines were firstly printed on Cardboard A, and they showed no conductivity. But from Figure 4(a), it can be observed that the edge of line is metallic, while the central area of the line pattern is black. Next, lines with multiple layers were printed on this substrate as a comparison. A normal method for fabricating multilayer patterns is printing multiple layers directly before sintering. The two-layer lines on Cardboard A were also dielectric, but the metallic area increased. Figure 4(b) shows that the eight-layer lines on Cardboard A become more metallic and the resistance is correspondingly lower, around 14 Ω. Based on the analyses above, it is apparent to summarize that the metallic part increases with the number of printed layers.

Table 3: Printing resolution of every substrate.

Substrate	Average drop size (μm)	Angle (degree)	Resolution (dpi)
Paper A	110	11.4	508
Paper B	90	9.1	635
Paper C	95	10.2	564
Cardboard A	90	9.1	635
Cardboard B	105	11.4	508

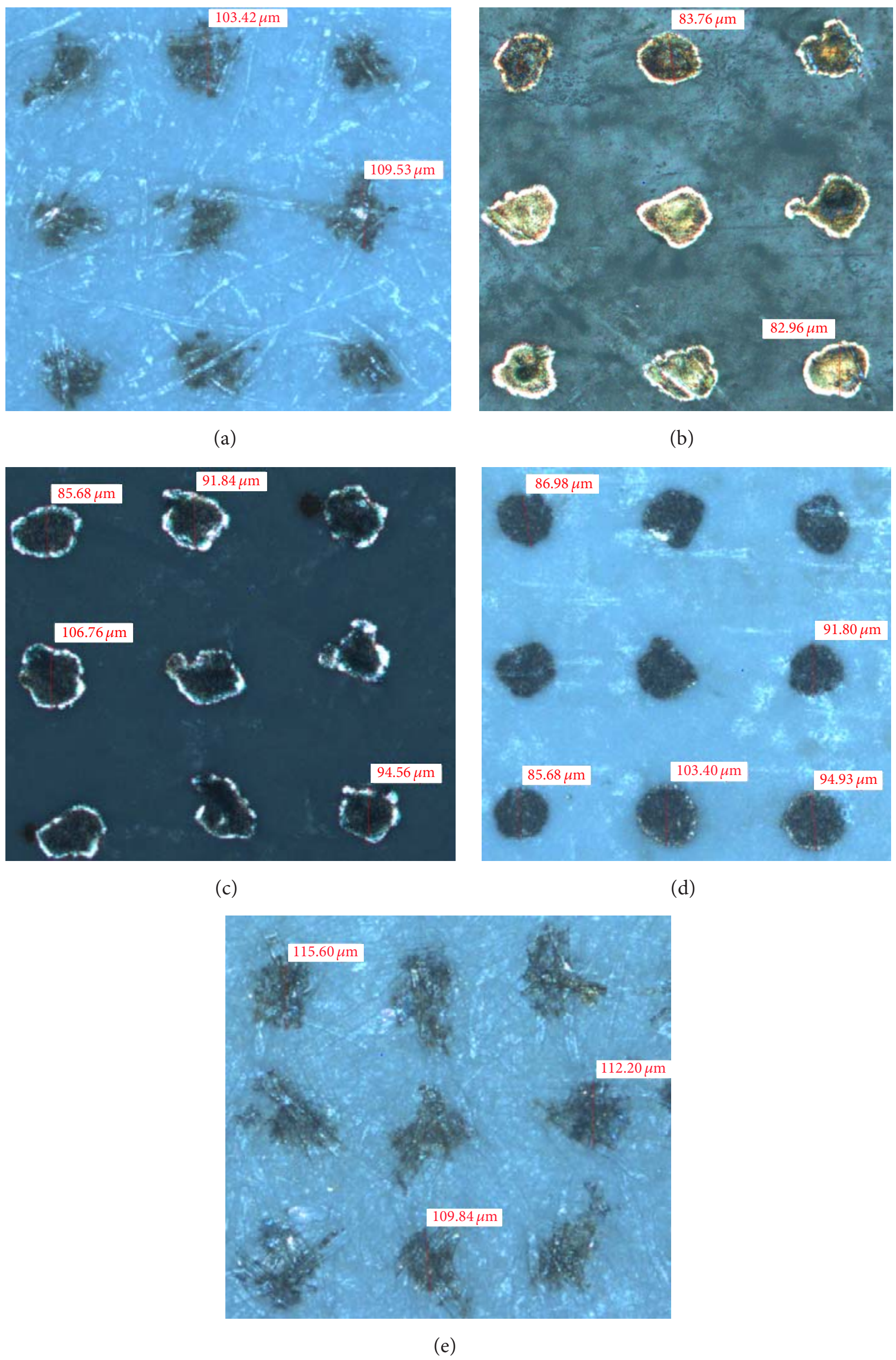

Figure 2: Droplet size test on all substrates: (a) droplets on Paper A, (b) droplets on Paper B, (c) droplets on Paper C, (d) droplets on Cardboard A, and (e) droplets on Cardboard B.

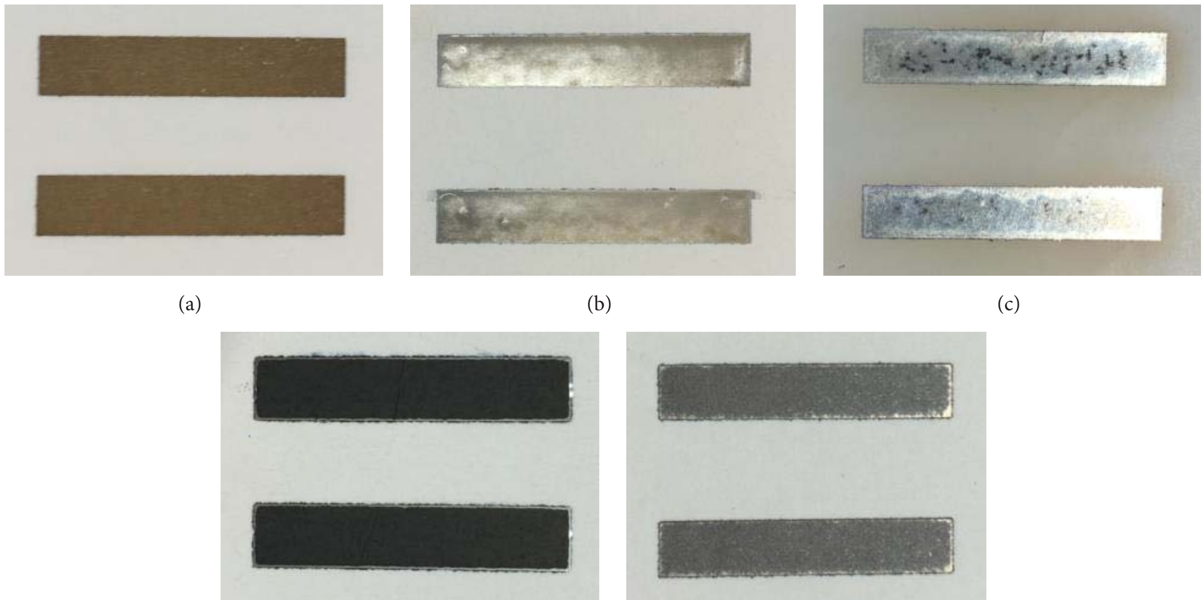

(a) (b) (c) (d) (e)

Figure 3: Inkjet-printed line patterns for fabrication optimization: (a) four-layer lines on Paper B, (b) four-layer lines on Paper A, (c) four-layer lines on Paper C, (d) four-layer lines on Cardboard A, and (e) four-layer lines on Cardboard B.

Table 4: Printing parameters.

Cartridge temperature (°C)	40
Platen temperature (°C)	50
Jetting voltage (V)	28
Jetting frequency (kHz)	23
Sintering time (minutes)	60
Sintering temperature (°C)	150

Another approach to manufacture the pattern with multiple layers is to repeat the process of printing and sintering. On this way, two printing-sintering rounds were carried out. At each turn, one-layer, two-layer, and four-layer lines were printed on Cardboard A and sintered in the oven. After that, the average resistance of those lines was measured, and they were found to be 5 Ω, 0.8 Ω, and 0.3 Ω, respectively. The major shortcoming of this method, along with the long manufacturing time, is that different layers are hard to be aligned perfectly.

The conductivity of the lines on Cardboard B was not good. The resistances of the four-layer lines and the eight-layer lines were found to be 2.5 MΩ and 161 Ω, respectively. Figure 4(c) shows the surface magnified image of the four-layer line, where the ink is absorbed by the substrate and the surface of the printed pattern is predominantly black with silver area inside. The metallic parts are not sufficient to form a good conductive trace, so the resistance is extremely high. Due to the poor performance, we chose not to try several printing-sintering rounds on Cardboard B.

On Paper A, the inkjet-printed lines showed no conductivity even with eight printed layers. The surface of the four-layer line is mostly black and no coherent metallic trace formed after sintering, which is shown in Figure 4(d) as an example. As with Cardboard B, due to the bad performance, we chose not to try several printing-sintering rounds.

On Paper B, the one-layer lines obtained good conductivity after sintering and the resistance was measured to be around 1.8 Ω. As shown in Figure 4(e), the surface is totally metallic although there are some small black holes and thin gaps. The possible reason is the inadequacy of the ink when only one layer is selected. As the number of the printed layers increases, the surface of the printed line becomes more homogenous. Thereby, the conductivity of the line increases with the number of layers. As the performance was excellent already after one layer, several printing-sintering rounds were not needed.

The two-layer lines on Paper C show tolerable conductivity as the average resistance is around 9.8 Ω, although the surface of the printed line is partially black, as shown in Figure 4(f). A continuous metallic pattern is formed when four layers and eight layers are applied. Again, multilayer printing brings much more ink and a greater thickness of silver film and therefore a lower resistance. As the performance was suitable already after four layers, several printing-sintering rounds were not needed.

2.4. Tag Fabrication Process. After finding the optimized printing parameters and the optimal number of layers, passive UHF RFID tag antennas were fabricated on Paper B, Paper C, Cardboard A, and Cardboard B. The tag antenna

Table 5: Resistances of printed lines on all substrates.

Substrate	Total layer(s)	Resistance (Ω)	Description
Paper A	2	∞	Not conductive, absorbed
	4	∞	Not conductive, absorbed
	8	∞	Not conductive, absorbed
Paper B	1	1.8	Good conductivity, totally metallic
	2	0.8	Good conductivity, totally metallic
	4	0.3	Good conductivity, totally metallic
Paper C	2	9.7	Good conductivity, mostly metallic
	4	2.8	Good conductivity, totally metallic
	6	2.1	Good conductivity, totally metallic
Cardboard A	1	∞	The edge of line is metallic, mostly black
	2	∞	The edge of line is metallic, mostly black
	4	79	The edge of line is metallic, mostly black
	6	14	The edge of line is metallic, mostly black
	8	1.3	The edge of line is metallic, partially black
	1-S-1	5	Totally silver, good conductivity
	2-S-2	0.8	Totally silver, good conductivity
	4-S-4	0.3	Totally silver, good conductivity
Cardboard B	2	∞	Not conductive
	4	2.5 M	Badly conductive
	8	161	Badly conductive

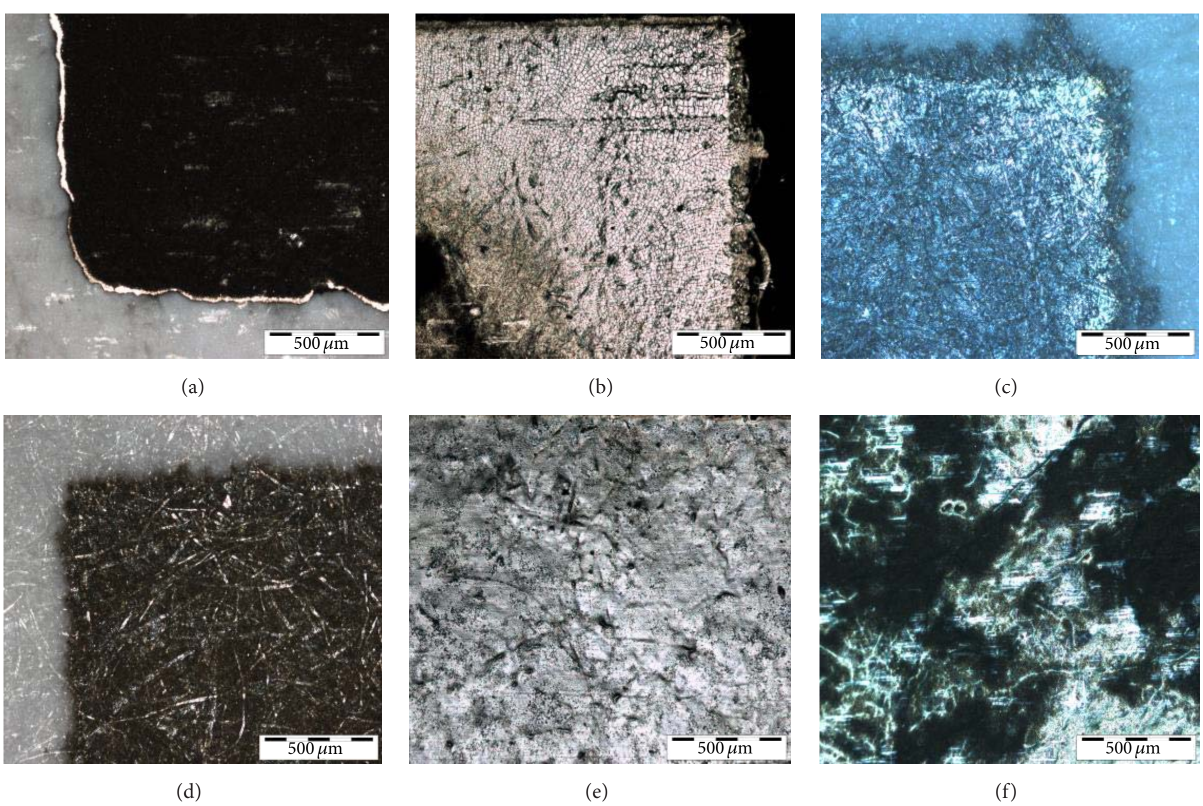

Figure 4: Microscopic images of the inkjet-printed layers: (a) surface of a one-layer line on Cardboard A, (b) surface of an eight-layer line on Cardboard A, (c) surface of a four-layer line on Cardboard B, (d) surface of a four-layer line on Paper A, (e) surface of a one-layer line on Paper B, and (f) surface of a two-layer line on Paper C.

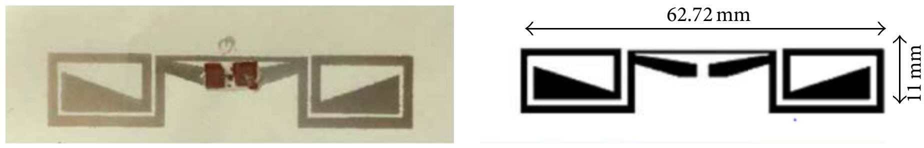

Figure 5: (a) A ready inkjet-printed UHF RFID tag on Paper B. (b) The utilized tag antenna geometry.

structure applied in this study is shown with a manufactured tag in Figure 5. As a typical dipole antenna layout, this geometric construction has been already successfully used in [12]. The sintering was done at 150°C for 60 minutes.

The used tag IC was NXP UCODE G2iL series RFID IC [13], provided by the manufacturer in a fixture patterned from copper on a plastic film. We attached the $3 \times 3\,\mathrm{mm}^2$ pads of the fixture to the printed antennas with CircuitWorks® Conductive Epoxy CW2400 [14], a highly reliable silver filled epoxy with a smooth, thixotropic consistency, and the IC-antenna joint was cured in 70°C for 20 minutes.

3. Measurements and Results

The wireless performance of the tags was evaluated with read range measurements using an RFID measurement unit. The tags were tested wirelessly using Voyantic Tagformance measurement system [15]. We conducted all the measurements with the tag suspended on a foam fixture in an anechoic chamber. The measurement equipment calculates the theoretical read range based on the measured path loss and the threshold power and computes the theoretical read range based on the relation given in

$$d = \frac{\lambda}{4\pi}\sqrt{\frac{\mathrm{EIRP}}{P_{\mathrm{th}} L_{\mathrm{iso}}}}, \tag{1}$$

where λ is the wavelength transmitted from the reader antenna, P_{th} is the measured threshold power, L_{iso} is the measured path loss, and EIRP is the emission limit of an RFID reader given as equivalent isotropic radiated power. We present all the results corresponding to EIRP = 3.28 W, which is the emission limit, for instance, in European countries.

As expected based on the resistance measurements, Paper B was found to be the most suitable substrate. As can be seen from Figure 6(a), the peak read ranges of the tags with only one layer are around 4 meters, which is already suitable for many practical applications. In addition, more layers lead to longer read ranges, since more ink was deposited on the paper to form a thicker conductive pattern, which has lower losses and better radiation efficiency. The 12-layer tags have the longest read ranges, and the peak was measured to be about 6.5 meters at around 940 MHz.

Figure 6(b) shows the read ranges of the multilayer tags on Paper C. First it indicates the same tendency that the read ranges increase together with the number of layers. However, the read ranges of the 12-layer tags are lower than the 8-layer tags, which have the best performance.

Judging from the data in Figure 6(c), the 6-layer tags on Cardboard A have the best performance and the peak read ranges can reach about 6.1 meters. After that, when more layers are printed, the read range decreases inversely.

Thus, depositing multiple layers directly does not always correspond to a higher read range and the optimized number of layers for antennas on each substrate material needs to be studied separately. In case of the tags printed on Cardboard A and Paper C, which were both double coated materials, the double coating most probably causes the substrate not to absorb as much ink as the other substrates. Thus, twelve printed layers are too much on these coated substrate materials, causing the read ranges to decrease compared to tags with eight or six printed layers. On paper-based porous substrates, the substrate will absorb some of the deposited ink. When depositing too much ink on the substrate, most probably the conductive layers are not as uniformly connected. In addition, the ink can spread and destroy the shape of the printed pattern. Thus, the read range will decrease when too many layers are printed.

The resistances of the printed lines on Cardboard B were very high. Also the performance of the tags on this substrate is unsatisfying. The read ranges of the inkjet-printed tags on Cardboard B are shown in Figure 6(d). The four-layer tags were firstly fabricated and obtained no response when measured. In addition, the peak read range of the eight-layer tag is only 2 meters. Next, 12-layer tags were manufactured by repeating printing and sintering process two times, and 6 layers were deposited at each round. The peak read range can reach 4 meters, which is sufficient for many applications. However, the manufacturing process cannot be considered to be efficient.

Generally, the dielectric substrate affects the tag performance through its electrical properties, such as loss tangent and relative permittivity. Porous substrates like paper and cardboard also have an indirect effect on the tag through the ink film morphology [6, 16]. The achieved results are very comparable to the earlier results with the same antenna geometry and silver nanoparticle ink in [12], where the tag antennas were fabricated by inkjet printing on a polyimide substrate (Kapton 200 HN [17]). Kapton is a low-loss, polyimide film, which provides a smooth, heat-resistant surface for high precision inkjet printing. The peak read range of a three-layer tag on polyimide was measured to be about 5.8 meters [12]. Thus, the environmentally friendly

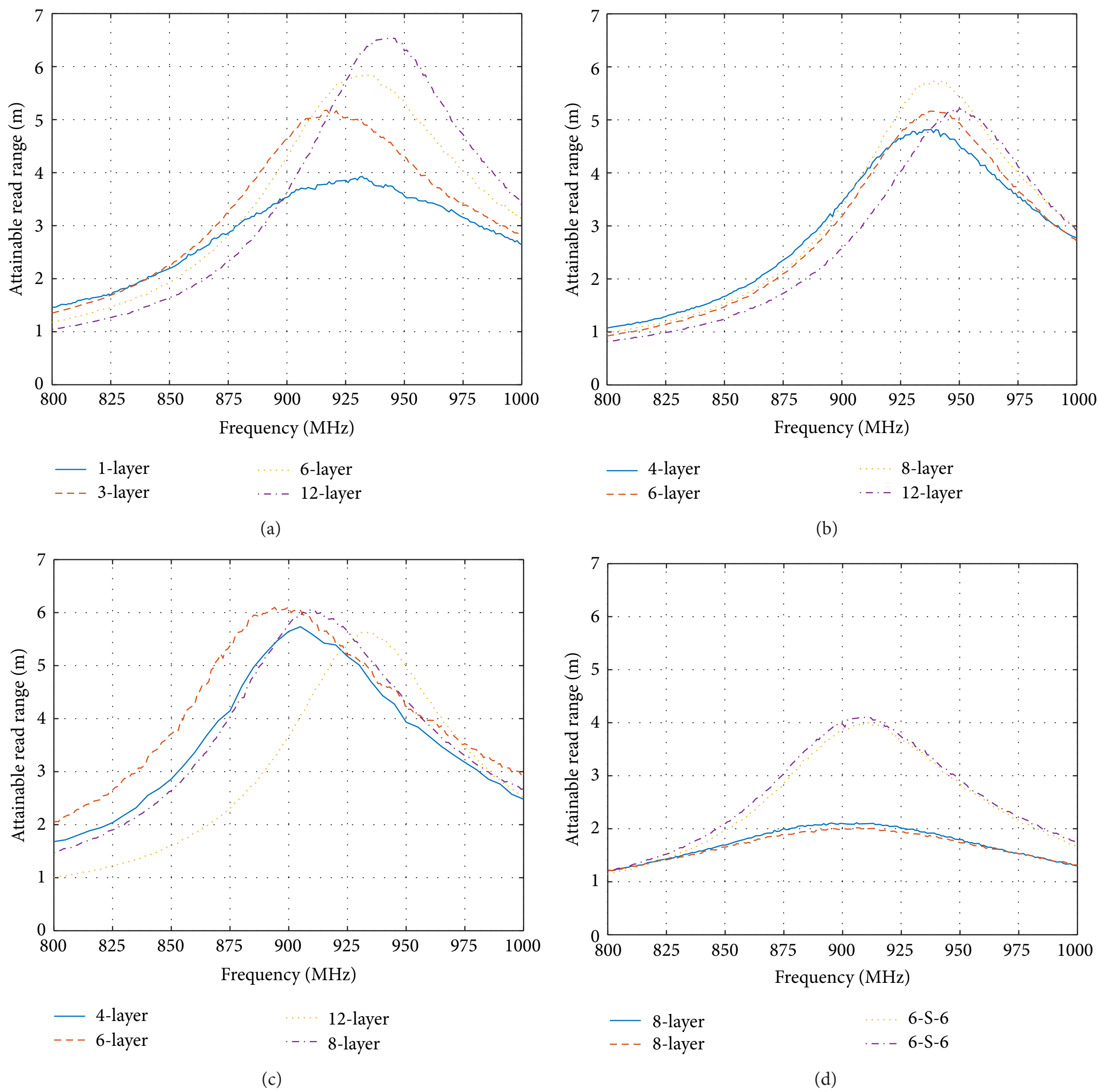

Figure 6: The measured read ranges of all tags: (a) the read ranges of tags on Paper B, (b) the read ranges of tags on Paper C, (c) the read ranges of tags on Cardboard A, and (d) the read ranges of tags on Cardboard B.

tags fabricated on these paper-based substrates in this study definitely have the potential to replace tags fabricated on traditionally used substrate materials and to be utilized in future wireless applications.

4. Conclusions

In this paper, the possibility of inkjet printing on versatile paper and cardboard substrates using silver nanoparticle ink was studied. The printing parameters were optimized for each substrate material in order to fabricate passive UHF RFID tags on these substrates. It was discovered that, in addition to the printing parameters, also the number of printed layers needs to be studied separately for each substrate material. The wireless performance of the fabricated tags was evaluated and the read ranges of the tags were found to be comparable to tags inkjet-printed on a polyimide substrate. In the future, the use of copper nanoparticle ink on these paper and cardboard substrates will be studied for potential cost reduction.

Competing Interests

The authors declare that there are no competing interests regarding the publication of this paper, and the mentioned received funding in Acknowledgments did not lead to any competing interests regarding its publication.

Acknowledgments

This research work was supported by the Academy of Finland and TEKES.

References

[1] G. Shaker, S. Safavi-Naeini, N. Sangary, and M. M. Tentzeris, "Inkjet printing of ultrawideband (UWB) antennas on paper-based substrates," *IEEE Antennas and Wireless Propagation Letters*, vol. 10, pp. 111–114, 2011.

[2] J. Virtanen, J. Virkki, L. Ukkonen, and L. Sydänheimo, "Inkjet-printed UHF RFID tags on renewable materials," *Advances in Internet Things*, vol. 2, no. 4, pp. 79–85, 2012.

[3] M. F. Farooqui and A. Shamim, "Dual band inkjet printed bow-tie slot antenna on leather," in *Proceedings of the 2013 7th European Conference on Antennas and Propagation (EuCAP '13)*, pp. 3287–3290, IEEE, Gothenburg, Sweden, April 2013.

[4] M. M. Tentzeris, L. Yang, A. Rida, A. Traille, R. Vyas, and T. Wu, "Inkjet-printed RFID tags on paper-based substrates for UHF 'cognitive intelligence' applications," in *Proceedings of the 18th Annual IEEE International Symposium on Personal, Indoor and Mobile Radio Communications (PIMRC '07)*, pp. 1–4, Athens, Greece, September 2007.

[5] L. Yang, A. Rida, R. Vyas, and M. M. Tentzeris, "RFID tag and RF structures on a paper substrate using inkjet-printing technology," *IEEE Transactions on Microwave Theory and Techniques*, vol. 55, no. 12, pp. 2894–2901, 2007.

[6] S. L. Merilampi, J. Virkki, L. Ukkonen, and L. Sydänheimo, "Testing the effects of temperature and humidity on printed passive UHF RFID tags on paper substrate," *International Journal of Electronics*, vol. 101, no. 5, pp. 711–730, 2014.

[7] R. Want, "An introduction to RFID technology," *IEEE Pervasive Computing*, vol. 5, no. 1, pp. 25–33, 2006.

[8] D. Dobkin, *The RF in RFID: Passive UHF RFID in Practice*, Elsevier, New York, NY, USA, 2007.

[9] N. C. Karmakar, Ed., *Handbook of Smart Antennas for RFID Systems*, John Wiley & Sons, Hoboken, NJ, USA, 2010.

[10] Harima Chemicals Group, "NPS-JL nanopaste, datasheet," http://www.harima.co.jp/en/products/.

[11] D. Soltman and V. Subramanian, "Inkjet-printed line morphologies and temperature control of the coffee ring effect," *Langmuir*, vol. 24, no. 5, pp. 2224–2231, 2008.

[12] J. Virtanen, J. Virkki, A. Z. Elsherbeni, L. Sydänheimo, and L. Ukkonen, "A selective ink deposition method for the cost-performance optimization of inkjet-printed UHF RFID tag antennas," *International Journal of Antennas and Propagation*, vol. 2012, Article ID 801014, 9 pages, 2012.

[13] NXP UCODE G2iL IC, Datasheet, http://www.nxp.com/documents/data_sheet/SL3S1203_1213.pdf.

[14] CircuitWorks® Conductive Epoxy, datasheet, https://www.chemtronics.com/descriptions/document/Cw2400tds.pdf.

[15] Voyantic Ltd, Tagformance, http://www.voyantic.com/tagformance.

[16] S. Merilampi, T. Björninen, A. Vuorimäki, L. Ukkonen, P. Ruuskanen, and L. Sydänheimo, "The effect of conductive ink layer thickness on the functioning of printed UHF RFID antennas," *Proceedings of the IEEE*, vol. 98, no. 9, pp. 1610–1619, 2010.

[17] DuPont HN Kapton, datasheet, http://www2.dupont.com/Kapton/en_US/assets/downloads/pdf/HN_datasheet.pdf.